European Journal of Pharmaceutical Sciences 195 (2024) 106720

Contents lists available at ScienceDirect

European Journal of Pharmaceutical Sciences

journal homepage: www.elsevier.com/locate/ejps

Predicting the intrinsic membrane permeability of Caco-2/MDCK cells by the solubility-diffusion model

Carolin Dahley [a], Tim Böckmann [a], Andrea Ebert [a,*], Kai-Uwe Goss [a,b]

[a] Department of Analytical Environmental Chemistry, Helmholtz Centre for Environmental Research (UFZ), Permoserstraße 15, Leipzig 04318, Germany
[b] Institute of Chemistry, University of Halle-Wittenberg, Kurt-Mothes-Straße 2, Halle 06120, Germany

ARTICLE INFO

Keywords:
Passive permeability
Intrinsic membrane permeability
Solubility-diffusion model
Black lipid membrane
Caco-2
MDCK

ABSTRACT

Membrane permeability is one of the main determinants for the absorption, distribution, metabolism and excretion of compounds and is therefore of crucial importance for successful drug development. Experiments with artificial phospholipid membranes have shown that the intrinsic membrane permeability (P_0) of compounds is well-predicted by the solubility-diffusion model (SDM). However, using the solubility-diffusion model to predict the P_0 of biological Caco-2 and MDCK cell membranes has proven unreliable so far. Recent publications revealed that many published P_0 extracted from Caco-2 and MDCK experiments are incorrect. In this work, we therefore used a small self-generated set as well as a large revised set of experimental Caco-2 and MDCK data from literature to compare experimental and predicted P_0. The P_0 extracted from Caco-2 and MDCK experiments were systematically lower than the P_0 predicted by the solubility-diffusion model. However, using the following correlation: $\log P_{0,\text{Caco-2/MDCK}} = 0.84 \log P_{0,\text{SDM}} - 1.85$, P_0 of biological Caco-2 and MDCK cell membranes was well-predicted by the solubility-diffusion model.

1. Introduction

Membrane permeability (P_m) is a crucial part of the ADME properties of a compound and therefore plays a key role in the pharmacokinetics and toxicokinetics of compounds (Di et al., 2020; Fagerholm, 2008). *In vitro* and *in silico* methods for predicting permeability have therefore become essential for effective drug development (O'Shea et al., 2022).

According to the pH-partition hypothesis, only the membrane permeability of the neutral fraction (f_n) of a compound is relevant. The permeability of the ionic fraction can usually be neglected (Ebert et al., 2018). For ionizable compounds, P_m is therefore dependent on pH. In order to enable a comparison between the P_m determined under different pH conditions, the pH-independent intrinsic membrane permeability of the neutral species (P_0) was introduced (Avdeef, 2001):

$$P_0 = \frac{P_m}{f_n} \tag{1}$$

In vitro, P_0 can be extracted from the apparent permeability (P_{app}) measured in cell-free (black lipid membrane (BLM) or parallel artificial membrane permeability assay (PAMPA)) or cell-based (Caco-2 or MDCK) permeability assays. These assays consist of a donor and an acceptor compartment separated by a barrier (O'Shea et al., 2022).

In BLM assays, the barrier is a single phospholipid bilayer with an adjacent aqueous boundary layer (ABL) on both sides. Assuming the same pH on both sides of the barrier (iso-pH method), $P_{0,BLM}$ can be calculated from $P_{app,BLM}$ as follows:

$$P_{0,BLM} = \frac{1}{\frac{1}{P_{app,BLM}} - \frac{1}{P_{ABL,BLM}}} \cdot \frac{1}{f_n} \tag{2}$$

In PAMPA, the phospholipid barrier is stabilized by a filter support, resulting in a reduced fragility. However, in contrast to BLM assays the structure of the phospholipid barrier in PAMPA is not known with certainty (Avdeef, 2012; Wohnsland and Faller, 2001) which might reduce the transferability to biological membranes. Therefore, PAMPA will not be further discussed in this paper.

In Caco-2 and MDCK assays, the barrier consists of a cell monolayer grown on a permeable filter support with an adjacent ABL on both sides. Compared to BLM assays, the extraction of $P_{0,\text{Caco-2/MDCK}}$ from $P_{app,\text{Caco-2/MDCK}}$ is more complex in Caco-2/MDCK assays, as more sub-processes contributing to $P_{app,\text{Caco-2/MDCK}}$ are involved. Caco-2/MDCK assays involve two membranes, apical and basolateral. Compared to the basolateral membrane, the surface area of the apical membrane is

* Corresponding author.
E-mail address: andrea.ebert@ufz.de (A. Ebert).

https://doi.org/10.1016/j.ejps.2024.106720
Received 20 November 2023; Received in revised form 17 January 2024; Accepted 1 February 2024
Available online 2 February 2024
0928-0987/© 2024 The Authors. Published by Elsevier B.V. This is an open access article under the CC BY license (http://creativecommons.org/licenses/by/4.0/).

increased by a factor of about 24 (Palay and Karlin, 1959) due to microvilli. Besides the ABL, additional aqueous barriers such as cytosol (cyt) and filter must be considered in the extraction of $P_{0,Caco\text{-}2/MDCK}$ from $P_{app,Caco\text{-}2/MDCK}$. Furthermore, paracellular transport (para) can occur in Caco-2/MDCK assays. The contributions of the individual sub-processes, in particular ABL and paracellular transport, differ substantially between different experimental setups, leading to a large interlaboratory variability of $P_{app,Caco\text{-}2/MDCK}$ (Lee et al., 2017). In comparison, the differences in $P_{0,Caco\text{-}2/MDCK}$ between different experimental setups are substantially smaller (Ebert et al., 2024). When the iso-pH method is used, the experimental $P_{0,Caco\text{-}2/MDCK}$ of a single membrane can be calculated from $P_{app,Caco\text{-}2/MDCK}$ according to Eq. (S1) in the Supporting Material.

Overall, the extraction of a reliable P_0 from P_{app} is only possible if the permeation process is dominated by the membrane. If the permeation process is dominated by aqueous barriers such as ABL, filter and cytosol or by paracellular transport extraction of a reliable P_0 is not possible.

Apart from the experimental (*in vitro*) methods summarized above, there are various predictive (*in silico*) approaches for determining P_0. Among them, quantitative structure-activity relationship (QSAR) models are purely empirical and not based on a mechanistic understanding of the permeation process. They are often trained on structurally similar molecules and therefore have limited transferability to structurally different molecules (Lomize et al., 2019).

A mechanistic approach for predicting permeability is the solubility-diffusion model (SDM) which regards the permeation process as a combination of consecutive diffusion and partitioning steps in the different layers of the membrane. Membranes are heterogeneous and consist of a polar headgroup region and a non-polar hydrocarbon core. However, for the majority of compounds, the hydrocarbon core consisting of long chain fatty acids is the main permeation resistance (Bittermann and Goss, 2017; Lomize and Pogozheva, 2019). Due to the chain length comparable to fatty acids, the hydrocarbon core is well modelled by hexadecane (Finkelstein, 1976; Walter and Gutknecht, 1986). Consequently, $P_{0,SDM}$ can be calculated from the diffusion coefficient of the compound in hexadecane (D_{hex}), the hexadecane-water partition coefficient ($K_{hex/w}$) and the thickness of the hexadecane-like hydrocarbon core (x_m):

$$P_{0,SDM} = \frac{D_{hex} \cdot K_{hex/w}}{x_m} \quad (3)$$

Ideally, all *in vitro* and *in silico* approaches should lead to the same P_0 for a given compound. Indeed, P_0 extracted from BLM experiments have proven to be well-predicted by the SDM over more than 7 orders of magnitude (Bittermann and Goss, 2017; Dahley et al., 2022). In contrast, our attempt to predict P_0 extracted from Caco-2/MDCK experiments by Avdeef (2012) with the SDM was unsuccessful, with deviations of several orders of magnitude for a large number of compounds (see Fig. 1). In order to further elucidate this problem, a direct comparison of experimental $P_{0,BLM}$ and $P_{0,Caco\text{-}2/MDCK}$ would be desirable, but P_0 was determined in both *in vitro* assays for only a small number of compounds. The existing data suggest that there are deviations between experimental $P_{0,BLM}$ and experimental $P_{0,Caco\text{-}2/MDCK}$ published by Avdeef (2012) that are particularly pronounced for lipophilic compounds (Dahley et al., 2022).

However, it has recently been shown that the dataset published by Avdeef (2012) contains a considerable number of incorrect experimental $P_{0,Caco\text{-}2/MDCK}$. Dahley et al. (2023) demonstrated that some experimental $P_{0,Caco\text{-}2/MDCK}$ are substantially too low because concentration-shift effects resulting from pH-differences in the Caco-2/MDCK assay were not considered. In addition to these concentration-shift effects, Ebert et al. (2024) recently identified further problems in the dataset of experimental $P_{0,Caco\text{-}2/MDCK}$ published by Avdeef (2012) and presented a revised and extended dataset of experimental $P_{0,Caco\text{-}2/MDCK}$.

Based on reliable experimental $P_{0,Caco\text{-}2/MDCK}$ we want to demonstrate that P_0 of biological membranes can be predicted by both BLM experiments and the SDM. As a starting point, we i) conducted our own MDCK and BLM transport experiments to extend the overlap between experimental $P_{0,MDCK}$ and $P_{0,BLM}$ and find a correlation between both methods and ii) compared $P_{0,MDCK}$ extracted from our own transport experiments and $P_{0,MDCK}$ predicted by BLM experiments to test the predictive power of the correlation. We then iii) compared $P_{0,MDCK}$ extracted from our own transport experiments and $P_{0,MDCK}$ predicted by the SDM to verify whether the correlation obtained for experimental BLM values is transferable to predicted SDM values. Lastly, we iv) compared $P_{0,Caco\text{-}2/MDCK}$ obtained from the revised dataset recently published by Ebert et al. (2024) and $P_{0,Caco\text{-}2/MDCK}$ predicted by the SDM to verify whether the correlation obtained in our laboratory is transferable to other laboratories.

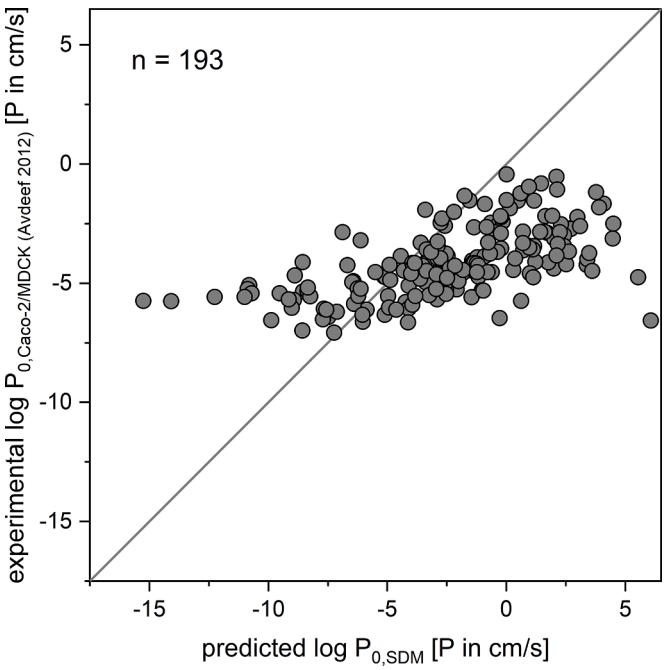

Fig. 1. Comparison of experimental log $P_{0,Caco\text{-}2/MDCK}$ and predicted log $P_{0,SDM}$. Experimental log $P_{0,Caco\text{-}2/MDCK}$ were obtained from Avdeef (2012). Predicted log $P_{0,SDM}$ were calculated from predicted $K_{hex/w}$ according to Eq. (3). Please note that for cefsulodine and cephaloridine prediction of log $P_{0,SDM}$ was not possible due to their permanent charge. The gray solid line represents the identity line.

2. Material and methods

2.1. Selection of compounds

For the extraction of $P_{0,BLM}$ and $P_{0,MDCK}$ from our own transport experiments, the 14 pharmaceutical compounds acebutolol, amantadine, chloroquine, diclofenac, fluvastatin, metoprolol, nadolol, pindolol, ranitidine, rizatriptan, salicylic acid, scopolamine, talinolol and venlafaxine were selected based on their diversity in predicted $P_{0,SDM}$. The respective suppliers are listed in Table S1 in the Supporting Material. For all selected compounds, it was ensured that the permeation process is dominated by the membrane and not by aqueous barriers (ABL, filter, cytosol) or paracellular transport, thus enabling the extraction of a reliable P_0.

Our own dataset of experimental $P_{0,MDCK}$ is extended by experimental $P_{0,Caco\text{-}2/MDCK}$ published by Ebert et al. (2024). Ebert et al. (2024) classified the $P_{0,Caco\text{-}2/MDCK}$ according to their reliability into the categories 1a, 1b, 2a and 2b. Compounds were classified in category 1 if no obvious problems occurred in the extraction of $P_{0,Caco\text{-}2/MDCK}$ from $P_{app,}$

$_{Caco\text{-}2/MDCK}$ and in category 2 if problems occurred (*e.g.* metabolism, uncertainty in pK_a, inconsistency between different references). In order to express the probability of $P_{0,Caco\text{-}2/MDCK}$ being affected by active transport, the letter 'a' was assigned to indicate that no active transport was detected in a bidirectional measurement or an inhibitor was used, while 'b' indicates more uncertain data where no action was taken to exclude active transport. In this paper, we focus on category 1a and 1b, which have the highest reliability.

2.2. Extraction of experimental $P_{0,BLM}$

$P_{app,BLM}$ was determined in BLM experiments with DPhPC membranes containing physiological amounts of cholesterol and sphingomyelin as described by Dahley et al. (2022). In brief, the painting-technique described by Mueller et al. (1963) was used to form black lipid membranes over an aperture (diameter: 1 mm), separating donor and acceptor compartment. Membrane formation and integrity was assured by electrical measurement of capacitance. The $P_{app,BLM}$ of the test compounds (5–100 μg/ml) at room temperature and at a stirring speed of 400 rpm was determined in a single-pH measurement using the iso-pH method. The following buffers were used to adjust the pH: 10 mM β-alanine (pH 4), 5 mM β-alanine and 5 mM MES (pH 5), 10 mM MES (pH 6), 10 mM MOPS (pH 7), 10 mM TAPS (pH 8–9) and 10 mM CAPSO (pH 10). Samples from the acceptor compartment were taken at regular time steps of 30 or 60 min and the sample volume was replaced with fresh buffer until the membrane collapsed or the capacitance was outside the specified range. The samples were analyzed using LC-MS/MS (Agilent Technologies Inc., Santa Clara, USA).

$P_{app,BLM}$ for amantadine, diclofenac, fluvastatin, metoprolol, nadolol, salicylic acid and venlafaxine were obtained from Dahley et al. (2022). $P_{app,BLM}$ for acebutolol, chloroquine, pindolol, ranitidine, rizatriptan, scopolamine and talinolol were determined in this work.

The method of determining $P_{0,BLM}$ from $P_{app,BLM}$ differs between Dahley et al. (2022) and this work in one aspect. In Dahley et al. (2022) we assumed the contribution of the ABL to be completely negligible. For higher accuracy, we consider the contribution of the ABL in this work and extract $P_{0,BLM}$ from $P_{app,BLM}$ according to Eq. (2). P_{ABL} can be calculated from the diffusion coefficient in water at 25 °C ($D_{w(25°C)}$), which is a function of molecular weight (MW) (Avdeef, 2010), and the experimentally determined ABL thickness (x_{ABL}) of 250 μm (Dahley et al., 2022):

$$P_{ABL} = \frac{D_{w(25°C)}}{x_{ABL}} \tag{4}$$

With:

$$D_{w(25°C)} = 10^{(-4.13-0.453\cdot\log(MW))} \tag{5}$$

The calculation of f_n for acids and bases can be found in Eqs. (S2)–(S5) in the Supporting Material. The pK_a values of all test compounds required for the calculation of f_n are listed in Table S2 in the Supporting Material.

For better comparability with experimental $P_{0,MDCK}$, the experimental $P_{0,BLM}$ values were adjusted in two aspects: (i) BLM assays were conducted at a room temperature of about 25 °C, while MDCK assays were conducted at 37 °C. Temperature differences result in differences in the diffusion coefficient. Compared to 25 °C, Avdeef et al. (2005) reported a 1.348-fold increase in the diffusion coefficient at 37 °C. Consequently, $P_{0,BLM}$ was multiplied by a temperature correction factor of 1.348. (ii) The thickness of the membrane interior is about 40 Å for the artificial BLM membranes used in this work (Dahley et al., 2022) and about 20 Å for biological membranes (Fettiplace et al., 1971). To account for the different thicknesses, $P_{0,BLM}$ was multiplied by a factor of 2.

2.3. Extraction of experimental $P_{0,MDCK}$

$P_{app,MDCK}$ was determined in MDCK transwell assays as described by Dahley et al. (2023) using the iso-pH method, which has proven to be advantageous over the gradient-pH method in the extraction of $P_{0,MDCK}$ (Dahley et al., 2023). In brief, MDCK-II-wildtype cells (The Netherlands Cancer Institute, Amsterdam, The Netherlands) were grown on 12-Well PET inserts (Cat. No. 9310402, CellQART, Northeim, Germany) for three days to form a confluent monolayer. In order to inhibit active transport, the inserts were preincubated with 2 μM elacridar prior to the transport experiments and 2 μM elacridar were added to the stock solutions of the test compounds. The apical-to-basolateral $P_{app,MDCK}$ of the test compounds (5–20 μg/ml) at a temperature 37 °C and a shaking speed of 450 rpm was determined either in a multiple-pH measurement or a single-pH measurement. The following buffers were used to adjust the pH: HBSS + 10 mM MES (pH 5–6.5), HBSS + 25 mM HEPES (pH 7–8) and HBSS + 10 mM TAPS (pH 8.5–9). Throughout the experiment, the pH was constant within a range of ± 0.2. The cell viability was not affected by pH (see Fig. S1 in the Supporting Material). Samples from the basolateral acceptor compartment were taken after 10, 20 and 30 min by completely replacing the basolateral buffer. Samples from the apical donor compartment were taken after 30 min to calculate recovery. The samples were analyzed using LC-MS/MS (Agilent Technologies Inc., Santa Clara, USA). Monolayer integrity was assured by measuring $P_{app,MDCK}$ of the paracellular marker Lucifer Yellow at pH 7.4 and the TEER for each individual insert (Dahley et al., 2023). The average $P_{app,MDCK}$ of Lucifer Yellow was $5.7 \pm 2 \times 10^{-7}$ cm/s and the average TEER was 139 ± 6 Ω cm^2 before the transport experiments and 140 ± 12 Ω cm^2 after the transport experiments.

$P_{0,MDCK}$ for amantadine, chloroquine and venlafaxine were obtained from Dahley et al. (2023) from a multiple-pH measurement of $P_{app,MDCK}$. $P_{0,MDCK}$ for ranitidine was determined accordingly in this work from a multiple-pH measurement of $P_{app,MDCK}$ at pH 5.0, 6.0, 7.0, 7.4, 8.0 and 9.0.

For acebutolol, diclofenac, fluvastatin, metoprolol, nadolol, pindolol, rizatriptan, salicylic acid, scopolamine and talinolol, $P_{app,MDCK}$ was determined in a single-pH measurement. The pH was chosen so that the membrane significantly contributes to $P_{app,MDCK}$, while the contribution of paracellular transport, ABL, filter and cytosol remains relatively small. $P_{0,MDCK}$ of a single membrane was extracted from $P_{app,MDCK}$ according to Eq. (S1) in the Supporting Material. P_{ABL}, P_{filter}, $S_{cyt}^{a\to b}$, P_{cyt} and f_n were calculated as described in detail by Dahley et al. (2023). P_{para} was estimated according to Avdeef and Tam (2010):

$$P_{para} = \frac{\varepsilon}{\delta} D_{w(37°C)} F\left(\frac{r}{R}\right) E(\Delta\varphi) + \frac{\varepsilon}{\delta_2} D_{w(37°C)} \tag{6}$$

Where ε/δ is the porosity-pathlength ratio of the first size-restricted and cation-selective pathway and ε/δ_2 is the porosity-pathlength ratio of the second size- and charge-independent pathway. $D_{w(37°C)}$ is the diffusion coefficient of the compound in water at 37 °C, F(r/R) is the Renkin hydrodynamic sieving function for cylindrical water channels and E(Δϕ) accounts for the potential drop across the electric field along the pores (Avdeef and Tam, 2010). For ε/δ, R and Δϕ we applied the parametrization determined for MDCK cells from the Netherlands Cancer Institute by Avdeef (2010). For ε/δ_2 we used 0.05 as described by Bittermann and Goss (2017). $D_{w(37°C)}$ was calculated according to Eq. (5) and multiplied by a factor of 1.348 to account for the temperature of 37 °C (Avdeef et al., 2005).

In order to check whether this method of calculating P_{para} is valid for our setup, we determined $P_{app,MDCK}$ of four paracellular markers, two acids (chlorothiazide, furosemide) and two bases (atenolol, sulpiride) (Avdeef, 2010). The pH was chosen to minimize the f_n and thus the transcellular transport of the compounds (pH 8.0 for acids and pH 5.0 for bases). It can therefore be assumed that the measured $P_{app,MDCK}$ was equal to P_{para}. Due to the low permeability, higher stock concentrations (20 μg/ml instead of 5–20 μg/ml) and longer sampling times (20, 40, 60

min instead of 10, 20, 30 min) were used for the determination of P_{para} compared to the determination of $P_{0,MDCK}$. Since the $P_{app,MDCK}$ of the two bases nadolol and ranitidine was relatively close to the calculated P_{para}, P_{para} was experimentally determined for both compounds under the same conditions as for the paracellular markers to increase the accuracy of the extracted $P_{0,MDCK}$. The comparison of experimental and calculated P_{para} shows that an adjustment factor of 1.67 for acids and 0.21 for bases needs to be included in the calculation of P_{para} for our setup (see Table S3 in the Supporting Material).

2.4. Prediction of $P_{0,SDM}$

$P_{0,SDM}$ was predicted according to Eq. (3). The diffusion coefficient in hexadecane (D_{hex}) was assumed to be one tenth of the diffusion coefficient in water at 37 °C ($D_{w(37°C)}$) (Bittermann and Goss, 2017). The thickness of the hexadecane-like membrane interior (x_m) was assumed to be 20 Å for biological membranes (Fettiplace et al., 1971). The hexadecane-water partition coefficient ($K_{hex/w}$) was predicted based on Linear Solvation Energy Relationship (LSER) descriptors using the UFZ-LSER database (Ulrich et al., 2017). Where available, experimental LSER descriptors were used, preferably from the "UFZ-preselected published values" dataset.

3. Results and discussion

3.1. Prediction of log $P_{0,MDCK}$ based on experimental log $P_{0,BLM}$

In order to obtain a reliable correlation between the P_0 extracted from different *in vitro* permeability assays, the P_0 of 14 pharmaceutical compounds was determined in our own BLM and MDCK experiments. A comparison between the resulting experimental log $P_{0,BLM}$ (see Table S4 in the Supporting Material) and experimental log $P_{0,MDCK}$ (see Table S5-S6 and Fig. S2 in the Supporting Material) is shown in Fig. 2.

Over a range of more than 6 orders of magnitude, there is a clear correlation between the log P_0 determined in both *in vitro* permeability assays for all compounds. However, it is not a 1:1 correlation. The

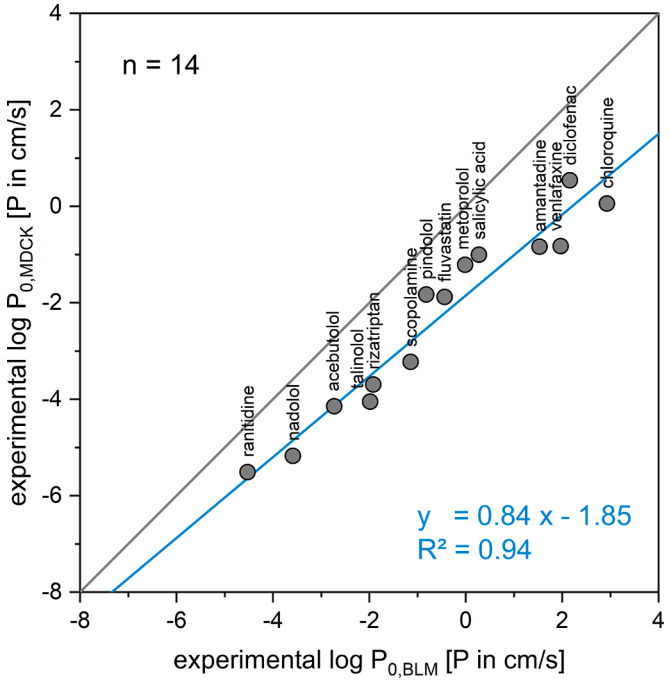

Fig. 2. Comparison of experimental log $P_{0,MDCK}$ and experimental log $P_{0,BLM}$. Experimental log $P_{0,MDCK}$ and log $P_{0,BLM}$ were determined in this work. The gray solid line represents the identity line. The blue solid line represents the regression line (log $P_{0,MDCK}$ = 0.84 log $P_{0,BLM}$ - 1.85).

experimentally determined log $P_{0,MDCK}$ are substantially lower than the experimentally determined log $P_{0,BLM}$. Performing a linear regression with OriginPro 2022 (OriginLab Corporation, Northampton, MA, USA), yields a slope of 0.84 ± 0.06 and an intercept of −1.85 ± 0.14 (R^2 = 0.94):

$$\log P_{0,MDCK} = 0.84 \log P_{0,BLM} - 1.85 \quad (7)$$

Thus, the regression function obtained from our data is in excellent agreement with the regression function obtained by Lomize and Pogozheva (2019), who found a slope of 0.81 and an intercept of -1.88 when comparing the experimental log P_0 of artificial (BLM and liposome) and biological (Caco-2, MDCK and blood-brain barrier) membranes.

The intercept of −1.85 ± 0.14 can be explained by differences in the composition of biological MDCK membranes and artificial BLM membranes. Lomize and Pogozheva (2019) hypothesized that the reduced permeability of biological membranes compared to artificial membranes might be attributed to cholesterol and sphingomyelin. Indeed, after addition of cholesterol to lecithin membranes a decrease in permeability of 0.6 to 1.1 log units was reported by Finkelstein (1976) and Xiang et al. (2000). However, the permeability-reducing effect of cholesterol appears to differ between different lipids and might be attenuated by sphingomyelin (Dahley et al., 2022). After addition of physiological amounts of cholesterol and sphingomyelin to DPhPC membranes, as in this work, no substantial change in permeability was observed (Dahley et al., 2022). In addition to the differences in lipid composition, biological membranes, unlike artificial membranes, contain proteins. Proteins decrease the accessible surface area (Di et al., 2012) and increase the membrane thickness (Mitra et al., 2004), resulting in a reduced permeability of biological membranes.

The slope of 0.84 ± 0.06 is close but not equal to the mechanistically expected slope of 1. For comparison, we therefore additionally performed a linear regression with a fixed slope of 1 (see Fig. S3 in the Supporting Material). Due to the higher accuracy, we decided to use the slope of 0.84 for the prediction of log $P_{0,MDCK}$ in the following plots. The plots using a fixed slope of 1 are shown in Figs. S4-S7 in the Supporting Material.

The experimental log $P_{0,MDCK}$ are plotted against the predicted log $P_{0,MDCK}$, calculated from experimental $P_{0,BLM}$ according to Eq. (7), in Fig. 3. The prediction exhibits a Root Mean Square Error (RMSE) of 0.48.

3.2. Prediction of log $P_{0,MDCK}$ based on predicted log $P_{0,SDM}$

Given that experimental $P_{0,BLM}$ have proven to be well-predicted by the SDM (Bittermann and Goss, 2017; Dahley et al., 2022), the correlation between predicted $P_{0,SDM}$ and experimental $P_{0,MDCK}$ is expected to be similar to the correlation between experimental $P_{0,BLM}$ and experimental $P_{0,MDCK}$ in Eq. (7). Indeed, plotting experimental log $P_{0,MDCK}$ against predicted log $P_{0,MDCK}$, calculated from predicted $P_{0,SDM}$ (see Table S7 in the Supporting Material) according to Eq. (7), reveals the same trend (see Fig. 4).

However, compared to Fig. 3, the scatter in Fig. 4 is substantially larger, which is reflected in a substantially higher RMSE of 1.14. This can be attributed to uncertainties in predicting $K_{hex/w}$, which is the critical input parameter in the SDM (see Eq. (3)). $K_{hex/w}$ is calculated based on Linear Solvation Energy Relationship (LSER) descriptors. The accuracy of the calculated $K_{hex/w}$ depends on the quality of the underlying LSER descriptors. In general, accuracy is substantially higher when experimental descriptors are used instead of predicted descriptors (Endo and Goss, 2014). Therefore, we mainly used compounds for which experimental descriptors are available. The sole exception where predicted descriptors were used is talinolol. Fig. 4 illustrates that talinolol is indeed the compound with the largest deviation between experimental and predicted log $P_{0,MDCK}$. Excluding the outlier talinolol, the RMSE decreases to 0.83. This underlines that experimental descriptors should be preferred over predicted descriptors. However, the quality of the

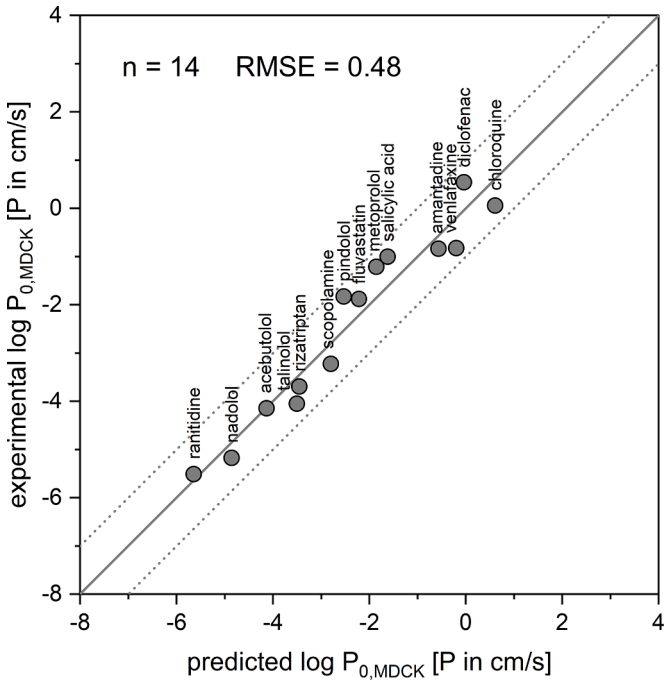

Fig. 3. Comparison of experimental log $P_{0,MDCK}$ and predicted log $P_{0,MDCK}$. Experimental log $P_{0,MDCK}$ were determined in this work. Predicted log $P_{0,MDCK}$ were calculated from experimental $P_{0,BLM}$ according to the equation: log $P_{0,MDCK}$ = 0.84 log $P_{0,BLM}$ - 1.85. The gray solid line represents the identity line, deviations of ±1 log unit are indicated as gray dotted lines.

experimental descriptors also varies among compounds, as it depends on the number, diversity and quality of the experimental partition coefficients used to calibrate the descriptors (Endo and Goss, 2014). It is imperative that these underlying experimental partition coefficients are explicitly determined for the neutral species, without any influence from the ionic species. Uncertainties concerning speciation are more likely to occur with dianions or dications, which might explain the pronounced deviation of the dication chloroquine from the identity line.

3.3. *Prediction of log $P_{0,Caco\text{-}2/MDCK}$ from literature based on predicted log $P_{0,SDM}$*

For a small dataset of 14 compounds, we were able to show that experimental $P_{0,MDCK}$ are well-predicted by the SDM. In order to find out whether this also applies to a larger dataset, experimental log $P_{0,Caco\text{-}2/MDCK}$ from the revised dataset published by Ebert et al. (2024) are plotted against predicted log $P_{0,Caco\text{-}2/MDCK}$, calculated from predicted $P_{0,SDM}$ according to Eq. (7), in Fig. 5. In order to reduce uncertainties, we only included compounds for which the experimental $P_{0,Caco\text{-}2/MDCK}$ was categorized as very reliable (categories 1a or 1b according to Ebert et al. (2024)) and for which experimental LSER descriptors are available. Plots that additionally include experimental $P_{0,Caco\text{-}2/MDCK}$ of low reliability (categories 2a and 2b according to Ebert et al. (2024)) and compounds for which only predicted LSER descriptors are available are shown in Fig. S8 in the Supporting Material.

Overall, there is good agreement between experimental and predicted log $P_{0,Caco\text{-}2/MDCK}$. As the examples of ranitidine, fluvastatin and chloroquine in Fig. 4 show, deviations of up to 1.5 log units between experimental and predicted log $P_{0,MDCK}$ can occur due to poor LSER descriptors and the associated uncertainties in $K_{hex/w}$. For the two compounds cyclosporin A and dopamine, the experimental log $P_{0,Caco\text{-}2/}$

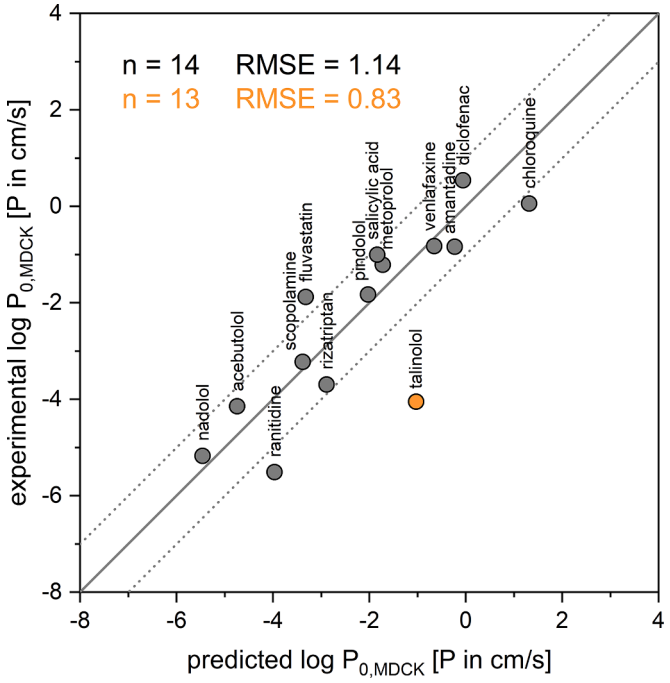

Fig. 4. Comparison of experimental log $P_{0,MDCK}$ and predicted log $P_{0,MDCK}$. Experimental $P_{0,MDCK}$ were determined in this work. Predicted log $P_{0,MDCK}$ were calculated from predicted $P_{0,SDM}$ according to the equation: log $P_{0,MDCK}$ = 0.84 log $P_{0,SDM}$ - 1.85. Predicted log $P_{0,SDM}$ were calculated from predicted $K_{hex/w}$ according to Eq. (3). Predicted $K_{hex/w}$ were calculated based on experimental and predicted LSER descriptors. The gray solid line represents the identity line, deviations of ±1 log unit are indicated as gray dotted lines. The RMSE including outliers is shown in black, the RMSE excluding outliers is shown in orange.

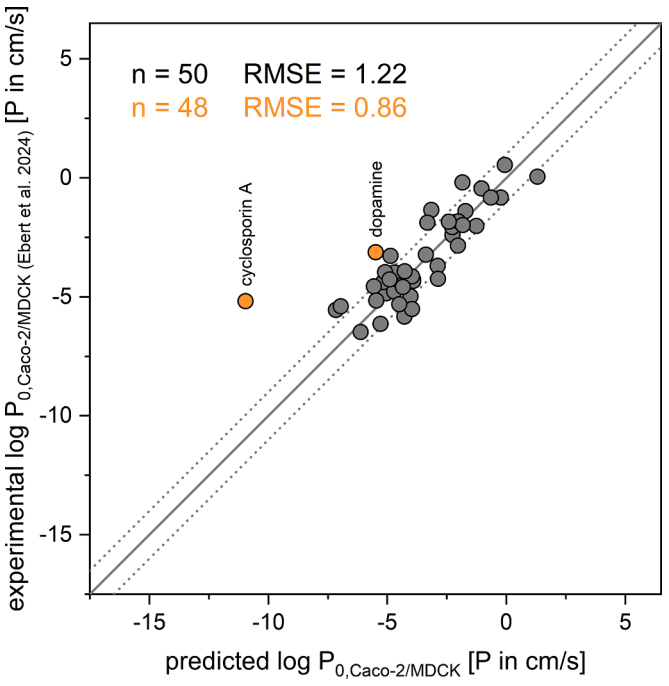

Fig. 5. Comparison of experimental log $P_{0,Caco\text{-}2/MDCK}$ and predicted log $P_{0,Caco\text{-}2/MDCK}$. Experimental log $P_{0,Caco\text{-}2/MDCK}$ of reliability category 1a and 1b were obtained from Ebert et al. (2024). Predicted log $P_{0,Caco\text{-}2/MDCK}$ were calculated from predicted log $P_{0,SDM}$ according to the equation: log $P_{0,Caco\text{-}2/MDCK}$ = 0.84 log $P_{0,SDM}$ - 1.85. Predicted log $P_{0,SDM}$ were calculated from predicted $K_{hex/w}$ according to Eq. (3). Predicted $K_{hex/w}$ were calculated based on experimental LSER descriptors. The gray solid line represents the identity line, deviations of ±1 log unit are indicated as gray dotted lines. The RMSE including outliers is shown in black, the RMSE excluding outliers is shown in orange.

MDCK deviates from the predicted log $P_{0,Caco\text{-}2/MDCK}$ by more than 2 log units. The fact that these compounds are outliers can be attributed to either an incorrectly predicted log $P_{0,SDM}$ resulting in an incorrectly predicted log $P_{0,Caco\text{-}2/MDCK}$ and/or an incorrect experimental log $P_{0,Caco\text{-}2/MDCK}$. Our first step in assessing the reliability of the predicted log $P_{0,SDM}$ was to compare it with experimental log $P_{0,BLM}$. Unfortunately, no experimental log $P_{0,BLM}$ is available for both outliers. Therefore, our second step in assessing the reliability of the predicted log $P_{0,SDM}$ was to compare the underlying $K_{hex/w}$ predicted from LSER descriptors to the $K_{hex/w}$ predicted by the alternative method COSMOthermX18 (COSMOlogic GmbH & Co KG, Leverkusen, Germany) (Eckert and Klamt, 2002). For cyclosporin A a log $K_{hex/w}$ of −11.17 resulting in a predicted log $P_{0,SDM}$ of −10.87 was calculated based on LSER descriptors, while a substantially higher log $K_{hex/w}$ of −4.44 resulting in a predicted log $P_{0,SDM}$ of −4.14 was calculated based on COSMOtherm. Assuming a predicted log $P_{0,SDM}$ of −4.14 for cyclosporin A based on the log $K_{hex/w}$ calculated with COSMOtherm, the experimental log $P_{0,Caco\text{-}2/MDCK}$ is in good agreement with the predicted log $P_{0,Caco\text{-}2/MDCK}$. For dopamine, there is no substantial difference between log $K_{hex/w}$ (LSER: -5.06, COSMOtherm: −4.71) and the resulting log $P_{0,SDM}$ (LSER: −4.35, COSMOtherm: −4.00) calculated with both methods, which might indicate that in the case of dopamine it is not the predicted $P_{0,SDM}$ but the experimental $P_{0,Caco\text{-}2/MDCK}$ that is incorrect. Although Ebert et al. (2024) took great care to eliminate the contribution of paracellular transport in the extraction of $P_{0,Caco\text{-}2/MDCK}$ from $P_{app,Caco\text{-}2/MDCK}$, experimental log $P_{0,Caco\text{-}2/MDCK}$ that are substantially above the identity line, as in the case of dopamine, but also cyclosporin A might indicate that these compounds are transported paracellularly and the extracted experimental log $P_{0,Caco\text{-}2/MDCK}$ are therefore incorrect. In order to estimate P_{para}, Ebert et al. (2024) used Eq. (6) which might be increasingly inaccurate for very small molecules such as dopamine (MW: 153.18 g/mol) and very large molecules such as cyclosporin A (MW: 1202.60 g/mol).

Fig. 5 confirms that the experimental log $P_{0,Caco\text{-}2/MDCK}$ of a large dataset of 50 compounds is well-predicted by the SDM, exhibiting an RMSE of 1.22 (including all compounds) or 0.86 (excluding the outliers cyclosporin A and dopamine). The RMSE obtained for literature data is almost identical to the RMSE obtained for in-house data, which proves the transferability of the prediction to the Caco-2 cell line and to other laboratories.

The accuracy of the prediction decreases with the quality of the LSER descriptors. Including compounds for which only predicted descriptors are available increased the RMSE from 1.22 to 1.35 (see Fig. S8A in the Supporting Material). Including compounds for which the experimental $P_{0,Caco\text{-}2/MDCK}$ was classified as category 2 due to problems in the extraction increased the RMSE more substantially from 1.22 to 1.54 (see Fig. S8B in the Supporting Material). A similar RMSE of 1.58 is obtained when all compounds are included regardless of the quality of their LSER descriptors or experimental $P_{0,Caco\text{-}2/MDCK}$ (see Fig. S8C in the Supporting Material). Thus, the degree of agreement between experimental and predicted $P_{0,Caco\text{-}2/MDCK}$ depends mainly on the quality of the experimental $P_{0,Caco\text{-}2/MDCK}$ and less on the quality of the LSER descriptors.

After showing that the experimental $P_{0,Caco\text{-}2/MDCK}$ published by Ebert et al. (2024) are well-predicted by the SDM, the question arises why the experimental $P_{0,Caco\text{-}2/MDCK}$ published by Avdeef (2012) deviate from the SDM for a large number of compounds (see Fig. 1). According to Ebert et al. (2024) the reason for this are incorrect experimental $P_{0,Caco\text{-}2/MDCK}$. As shown in Fig. 6, about 25 % of the compounds selected by Avdeef (2012) are zwitterions. For zwitterions, Avdeef (2012) assumed in most cases that the permeability of the zwitterionic species is equal to the permeability of the neutral species of a compound. However, studies with amino acids indicate that the permeability of the zwitterionic species might be substantially lower than the permeability of the neutral species and therefore both species cannot be treated equally (Chakrabarti and Deamer, 1992). For about 30 % of the compounds, the experimental $P_{0,Caco\text{-}2/MDCK}$ reported by Avdeef (2012) are too low

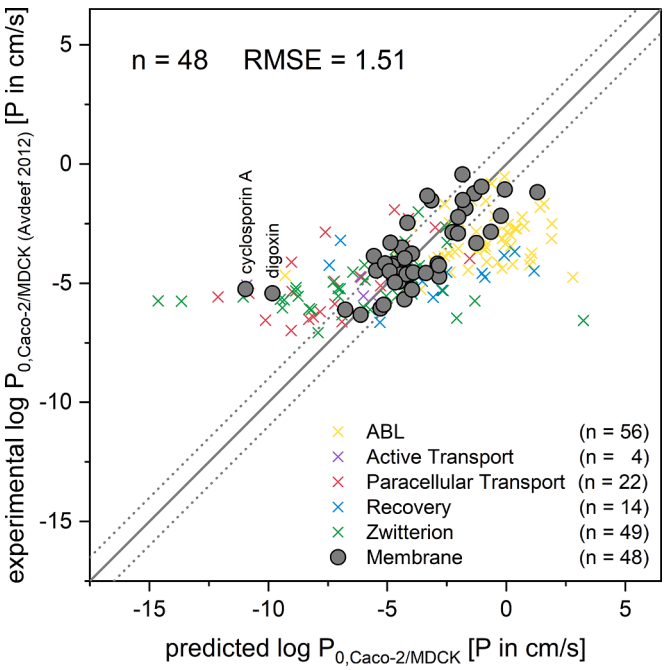

Fig. 6. Comparison of experimental log $P_{0,Caco\text{-}2/MDCK}$ and predicted log $P_{0,Caco\text{-}2/MDCK}$. Circles represent compounds for which extraction of a reliable experimental log $P_{0,Caco\text{-}2/MDCK}$ is possible due to membrane-limitation of the underlying $P_{app,Caco\text{-}2/MDCK}$ (n = 48). Crosses represent compounds for which extraction of a reliable experimental log $P_{0,Caco\text{-}2/MDCK}$ is not possible (n = 145). Experimental log $P_{0,Caco\text{-}2/MDCK}$ were obtained from Avdeef (2012). Predicted log $P_{0,Caco\text{-}2/MDCK}$ were calculated from predicted $P_{0,SDM}$ according to the equation: log $P_{0,Caco\text{-}2/MDCK}$ = 0.84 log $P_{0,SDM}$ - 1.85. Predicted log $P_{0,SDM}$ were calculated from predicted $K_{hex/w}$ according to Eq. (3). Predicted $K_{hex/w}$ were calculated based on experimental and predicted LSER descriptors. Please note that for cefsulodine and cephaloridine prediction of log $P_{0,SDM}$ was not possible due to their permanent charge. The gray solid line represents the identity line, deviations of ±1 log unit are indicated as gray dotted lines.

because the underlying $P_{app,Caco\text{-}2/MDCK}$ was dominated by the ABL. About 10 % of the reported experimental $P_{0,Caco\text{-}2/MDCK}$ are too high because the underlying $P_{app,Caco\text{-}2/MDCK}$ was dominated by paracellular transport. In addition, some compounds are transported actively or recovery issues occurred due to high lipophilicity, which negatively affects the extraction of a reliable experimental $P_{0,Caco\text{-}2/MDCK}$.

For only 25 % of the selected compounds, $P_{app,Caco\text{-}2/MDCK}$ is dominated by the membrane and thus a reliable experimental $P_{0,Caco\text{-}2/MDCK}$ can be extracted. With the exception of cyclosporin A and digoxin, these remaining reliable experimental $P_{0,Caco\text{-}2/MDCK}$ are no longer in contradiction with the $P_{0,Caco\text{-}2/MDCK}$ predicted by the SDM. Analogous to the deviation of cyclosporin A discussed previously, the deviation of digoxin can be attributed to uncertainties in the predicted $K_{hex/w}$ and the associated predicted $P_{0,Caco\text{-}2/MDCK}$ and uncertainties in the estimated P_{para} for molecules with high molecular weight and the associated experimental $P_{0,Caco\text{-}2/MDCK}$. The experimental $P_{0,Caco\text{-}2/MDCK}$ extracted by Avdeef (2012) differ in most cases by less than one log unit from the experimental $P_{0,Caco\text{-}2/MDCK}$ extracted by Ebert et al. (2024). This is reflected in an RMSE of 1.51, which is comparable to the RMSE of 1.58 obtained for the data from Ebert et al. (2024) including all compounds regardless of the quality of the experimental $P_{0,Caco\text{-}2/MDCK}$ or LSER descriptors (see Fig. S8C in the Supporting Material). Avdeef (2012) and Ebert et al. (2024) thus hardly differ in the experimental $P_{0,Caco\text{-}2/MDCK}$ extracted from membrane-dominated $P_{app,Caco\text{-}2/MDCK}$, but rather in which $P_{app,Caco\text{-}2/MDCK}$ are considered as membrane-dominated. The application of stricter exclusion criteria by Ebert et al. (2024) was necessary to generate a more reliable dataset. However, due to the stricter exclusion criteria, there might be compounds among the

excluded compounds for which the $P_{app,Caco\text{-}2/MDCK}$ was classified as limited by the ABL or paracellular transport, although an extraction of $P_{0,Caco\text{-}2/MDCK}$ might still have been possible. This might explain why the experimental log $P_{0,Caco\text{-}2/MDCK}$ of some excluded compounds is nevertheless in good agreement with the predicted log $P_{0,Caco\text{-}2/MDCK}$.

4. Conclusion

In this work, we introduced a fast, simple and reliable method for predicting $P_{0,Caco\text{-}2/MDCK}$ based on experimental $P_{0,BLM}$ or predicted $P_{0,SDM}$ (see Eq. (7)). The accuracy of the predicted $P_{0,Caco\text{-}2/MDCK}$ was evaluated against experimental $P_{0,MDCK}$ obtained from our own transport experiments (RMSE = 0.48 based on experimental $P_{0,BLM}$, RMSE = 0.83 based on predicted $P_{0,SDM}$) and revised experimental $P_{0,Caco\text{-}2/MDCK}$ obtained from Ebert et al. (2024) (RMSE = 0.86 based on predicted $P_{0,SDM}$). The accuracy of the predicted $P_{0,SDM}$ is determined by $K_{hex/w}$. In this work $K_{hex/w}$ was calculated from LSER descriptors and therefore substantially depends on the quality of the underlying LSER descriptors. Due to the higher reliability, experimental LSER descriptors should be used. However, for a rough estimation of $P_{0,Caco\text{-}2/MDCK}$, our model works sufficiently well with predicted LSER descriptors (RMSE = 1.35).

A reliable prediction of $P_{0,Caco\text{-}2/MDCK}$ enables modelling of P_{app} in different *in vitro* and *in vivo* scenarios (different ABL thicknesses, different paracellular transport, different pH conditions). Our model can therefore be used to systematically screen the permeability of potential drug candidates through biological membrane in early drug discovery. It enables the computational determination of $P_{0,Caco\text{-}2/MDCK}$ for compounds for which an experimental determination of $P_{0,Caco\text{-}2/MDCK}$ *in vitro* is not possible, *e.g.* for hydrophobic compounds due to ABL limitation. Furthermore it serves as a useful tool for optimizing the setup for the experimental determination of reliable $P_{0,Caco/MDCK}$. However, it should be noted that our model is only applicable to compounds for which the non-polar hydrocarbon core and not the polar headgroup region of the membrane is the limiting barrier for permeation. Thus, the permeability of compounds that are more hydrophobic than those discussed in this work might be overestimated by our prediction.

Funding

This research did not receive any specific grant from funding agencies in the public, commercial, or not-for-profit sectors.

CRediT authorship contribution statement

Carolin Dahley: Formal analysis, Investigation, Methodology, Visualization, Writing – original draft. **Tim Böckmann:** Investigation, Writing – review & editing. **Andrea Ebert:** Formal analysis, Writing – review & editing. **Kai-Uwe Goss:** Conceptualization, Supervision, Writing – review & editing.

Declaration of competing interest

The authors declare that they have no known competing financial interests or personal relationships that could have appeared to influence the work reported in this paper.

Data availability

Data will be made available on request.

Supplementary materials

Supplementary material associated with this article can be found, in the online version, at doi:10.1016/j.ejps.2024.106720.

References

Avdeef, A., 2001. Physicochemical profiling (solubility, permeability and charge state). Curr. Top. Med. Chem. 1 (4), 277–351. https://doi.org/10.2174/1568026013395100.

Avdeef, A., 2010. Leakiness and size exclusion of paracellular channels in cultured epithelial cell monolayers-interlaboratory comparison. Pharm. Res. 27 (3), 480–489. https://doi.org/10.1007/s11095-009-0036-7.

Avdeef, A., 2012. Absorption and Drug development: Solubility, permeability, and Charge State, 2nd ed. John Wiley & Sons, Hoboken N.J.

Avdeef, A., Artursson, P., Neuhoff, S., Lazorova, L., Gråsjö, J., Tavelin, S., 2005. Caco-2 permeability of weakly basic drugs predicted with the double-sink PAMPA pKa(flux) method. Eur. J. Pharm. Sci. 24 (4), 333–349. https://doi.org/10.1016/j.ejps.2004.11.011.

Avdeef, A., Tam, K.Y., 2010. How well can the Caco-2/Madin-Darby canine kidney models predict effective human jejunal permeability? J. Med. Chem. 53 (9), 3566–3584. https://doi.org/10.1021/jm901846t.

Bittermann, K., Goss, K.U., 2017. Predicting apparent passive permeability of Caco-2 and MDCK cell-monolayers: a mechanistic model. PLoS. One 12 (12), e0190319. https://doi.org/10.1371/journal.pone.0190319.

Chakrabarti, A.C., Deamer, D.W., 1992. Permeability of lipid bilayers to amino acids and phosphate. Biochim. Biophys. Acta Biomembr. 1111 (2), 171–177. https://doi.org/10.1016/0005-2736(92)90308-9.

Dahley, C., Garessus, E.D.G., Ebert, A., Goss, K.U., 2022. Impact of cholesterol and sphingomyelin on intrinsic membrane permeability. Biochim. Biophys. Acta Biomembr. 1864 (9), 183953 https://doi.org/10.1016/j.bbamem.2022.183953.

Dahley, C., Goss, K.U., Ebert, A., 2023. Revisiting the pKa-Flux method for determining intrinsic membrane permeability. Eur. J. Pharm. Sci. 191, 106592 https://doi.org/10.1016/j.ejps.2023.106592.

Di, L., Artursson, P., Avdeef, A., Benet, L.Z., Houston, J.B., Kansy, M., Kerns, E.H., Lennernäs, H., Smith, D.A., Sugano, K., 2020. The critical role of passive permeability in designing successful drugs. ChemMedChem. 15 (20), 1862–1874. https://doi.org/10.1002/cmdc.202000419.

Di, L., Artursson, P., Avdeef, A., Ecker, G.F., Faller, B., Fischer, H., Houston, J.B., Kansy, M., Kerns, E.H., Krämer, S.D., Lennernäs, H., Sugano, K., 2012. Evidence-based approach to assess passive diffusion and carrier-mediated drug transport. Drug Discov. Today 17 (15–16), 905–912. https://doi.org/10.1016/j.drudis.2012.03.015.

Ebert, A., Dahley, C., Goss, K.U., 2024. Pitfalls in evaluating permeability experiments with Caco-2/MDCK cell monolayers. Eur. J. Pharm. Sci 194, 106699. https://doi.org/10.1016/j.ejps.2024.106699.

Ebert, A., Hannesschlaeger, C., Goss, K.U., Pohl, P., 2018. Passive permeability of planar lipid bilayers to organic anions. Biophys. J. 115 (10), 1931–1941. https://doi.org/10.1016/j.bpj.2018.09.025.

Eckert, F., Klamt, A., 2002. Fast solvent screening via quantum chemistry: COSMO-RS approach. AIChe J. 48 (2), 369–385. https://doi.org/10.1002/aic.690480220.

Endo, S., Goss, K.U., 2014. Applications of polyparameter linear free energy relationships in environmental chemistry. Environ. Sci. Technol. 48 (21), 12477–12491. https://doi.org/10.1021/es503369t.

Fagerholm, U., 2008. The role of permeability in drug ADME/PK, interactions and toxicity—presentation of a permeability-based classification system (PCS) for prediction of ADME/PK in humans. Pharm. Res. 25 (3), 625–638. https://doi.org/10.1007/s11095-007-9397-y.

Fettiplace, R., Andrews, D.M., Haydon, D.A., 1971. The thickness, composition and structure of some lipid bilayers and natural membranes. J. Membr. Biol. 5 (3), 277–296. https://doi.org/10.1007/BF01870555.

Finkelstein, A., 1976. Water and nonelectrolyte permeability of lipid bilayer membranes. J. Gen. Physiol. 68 (2), 127–135. https://doi.org/10.1085/jgp.68.2.127.

Lee, J.B., Zgair, A., Taha, D.A., Zang, X., Kagan, L., Kim, T.H., Kim, M.G., Yun, H., Fischer, P.M., Gershkovich, P., 2017. Quantitative analysis of lab-to-lab variability in Caco-2 permeability assays. Eur. J. Pharm. Biopharm. 114, 38–42. https://doi.org/10.1016/j.ejpb.2016.12.027.

Lomize, A.L., Hage, J.M., Schnitzer, K., Golobokov, K., LaFaive, M.B., Forsyth, A.C., Pogozheva, I.D., 2019. PerMM: a web tool and database for analysis of passive membrane permeability and translocation pathways of bioactive molecules. J. Chem. Inf. Model. 59 (7), 3094–3099. https://doi.org/10.1021/acs.jcim.9b00225.

Lomize, A.L., Pogozheva, I.D., 2019. Physics-based method for modeling passive membrane permeability and translocation pathways of bioactive molecules. J. Chem. Inf. Model. 59 (7), 3198–3213. https://doi.org/10.1021/acs.jcim.9b00224.

Mitra, K., Ubarretxena-Belandia, I., Taguchi, T., Warren, G., Engelman, D.M., 2004. Modulation of the bilayer thickness of exocytic pathway membranes by membrane proteins rather than cholesterol. Proc. Natl. Acad. Sci. U. S. A. 101 (12), 4083–4088. https://doi.org/10.1073/pnas.0307332101.

Mueller, P., Rudin, D.O., Tien, H.T., Wescott, W.C., 1963. Methods for the formation of single bimolecular lipid membranes in aqueous solution. J. Phys. Chem. 67 (2), 534–535. https://doi.org/10.1021/j100796a529.

O'Shea, J.P., Augustijns, P., Brandl, M., Brayden, D.J., Brouwers, J., Griffin, B.T., Holm, R., Jacobsen, A.C., Lennernäs, H., Vinarov, Z., O'Driscoll, C.M., 2022. Best practices in current models mimicking drug permeability in the gastrointestinal tract - an UNGAP review. Eur. J. Pharm. Sci. 170, 106098 https://doi.org/10.1016/j.ejps.2021.106098.

Palay, S.L., Karlin, L.J., 1959. An electron microscopic study of the intestinal villus: II. the pathway of fat absorption. J. Biophys. Biochem. Cytol. 5 (3), 373–384. https://doi.org/10.1083/jcb.5.3.373.

Ulrich N., Endo S., Brown T.N., Watanabe N., Bronner G., Abraham M.H., Goss K.U., 2017. UFZ-LSER database v3.2.1. http://www.ufz.de/lserd. [Accessed 11 October 2023].

Walter, A., Gutknecht, J., 1986. Permeability of small nonelectrolytes through lipid bilayer membranes. J. Membr. Biol. 90 (3), 207–217. https://doi.org/10.1007/BF01870127.

Wohnsland, F., Faller, B., 2001. High-throughput permeability pH profile and high-throughput alkane/water log P with artificial membranes. J. Med. Chem. 44 (6), 923–930. https://doi.org/10.1021/jm001020e.

Xiang, T.X., Chen, J., Anderson, B.D., 2000. A quantitative model for the dependence of solute permeability on peptide and cholesterol content in biomembranes. J. Membr. Biol. 177 (2), 137–148. https://doi.org/10.1007/s002320001107.